

Retrospective Study

Diagnostic performance of abbreviated gadoxetic acid-enhanced magnetic resonance protocols with contrast-enhanced computed tomography for detection of colorectal liver metastases

Kumi Ozaki, Shota Ishida, Shohei Higuchi, Toyohiko Sakai, Ayaki Kitano, Kenji Takata, Kazuyuki Kinoshita, Yuki Matta, Takashi Ohtani, Hirohiko Kimura, Toshifumi Gabata

Specialty type: Gastroenterology and hepatology

Provenance and peer review: Invited article; Externally peer reviewed.

Peer-review model: Single blind

Peer-review report's scientific quality classification

Grade A (Excellent): 0
Grade B (Very good): B
Grade C (Good): 0
Grade D (Fair): D
Grade E (Poor): 0

P-Reviewer: Gao L, China; Liao W, China

Received: August 14, 2022

Peer-review started: August 14, 2022

First decision: August 29, 2022

Revised: September 5, 2022

Accepted: October 5, 2022

Article in press: October 5, 2022

Published online: October 28, 2022



Kumi Ozaki, Shohei Higuchi, Toyohiko Sakai, Ayaki Kitano, Kenji Takata, Kazuyuki Kinoshita, Yuki Matta, Takashi Ohtani, Hirohiko Kimura, Department of Radiology, University of Fukui, Fukui 9101193, Japan

Shota Ishida, Department of Radiological Technology, Faculty of Medical Science, Kyoto College of Medical Science, Kyoto 6220041, Japan

Toshifumi Gabata, Department of Radiology, Kanazawa University Graduate School of Medical Science, Kanazawa 9208641, Japan

Corresponding author: Kumi Ozaki, MD, PhD, Lecturer, Department of Radiology, University of Fukui, 23-3 Matsuoka-Shimoaizuki, Fukui 9101193, Japan. ozakik-rad@umin.org

Abstract

BACKGROUND

Although contrast-enhanced magnetic resonance imaging (MRI) using gadoxetic acid has been shown to have higher accuracy, sensitivity, and specificity for the detection and characterization of hepatic metastases compared with other modalities, the long examination time would limit the broad indication. Several abbreviated enhanced MRI (Ab-MRI) protocols without dynamic phases have been proposed to achieve equivalent diagnostic performance for the detection of colorectal liver metastases. However, an optimal protocol has not been established, and no studies have assessed the diagnostic performance of Ab-MRI combined with contrast-enhanced computed tomography (CE-CT), which is the preoperative imaging of colorectal cancer staging in clinical settings, to determine the best therapeutic strategy.

AIM

To compare the diagnostic performance of two kinds of Ab-MRI protocol with the standard MRI protocol and a combination of the Ab-MRI protocol and CE-CT for the detection of colorectal liver metastases.

METHODS

Study participants comprised 87 patients (51 males, 36 females; mean age, 67.2 ± 10.8 years) who had undergone gadoxetic acid-enhanced MRI and CE-CT during

the initial work-up for colorectal cancer from 2010 to 2021. Each exam was independently reviewed by two readers in three reading sessions: (1) Only single-shot fast spin echo (FSE) T2-weighted or fat-suppressed-FSE-T2-weighted, diffusion-weighted, and hepatobiliary-phase images (Ab-MRI protocol 1 or 2); (2) all acquired MRI sequences (standard protocol); and (3) a combination of an Ab-MRI protocol (1 or 2) and CE-CT. Diagnostic performance was then statistically analyzed.

RESULTS

A total of 380 Lesions were analyzed, including 195 metastases (51.4%). Results from the two Ab-MRI protocols were similar. The sensitivity, specificity, and positive and negative predictive values from Ab-MRI were non-inferior to those from standard MRI ($P > 0.05$), while those from the combination of Ab-MRI protocol and CE-CT tended to be higher than those from Ab-MRI alone, although the difference was not significant ($P > 0.05$), and were quite similar to those from standard MRI ($P > 0.05$).

CONCLUSION

The diagnostic performances of two Ab-MRI protocols were non-inferior to that of the standard protocol. Combining Ab-MRI with CE-CT provided better diagnostic performance than Ab-MRI alone.

Key Words: Colorectal liver metastases; Gadoxetic acid; Magnetic resonance imaging; Hepatobiliary phase; Contrast-enhanced computed tomography; Diagnostic performance

©The Author(s) 2022. Published by Baishideng Publishing Group Inc. All rights reserved.

Core Tip: For the detection of colorectal liver metastases, the diagnostic performance of two kinds of abbreviated enhanced magnetic resonance imaging (Ab-MRI) protocols was non-inferior to that of the standard protocol. The combination of Ab-MRI and contrast-enhanced computed tomography provided better diagnostic performance than that of Ab-MRI alone.

Citation: Ozaki K, Ishida S, Higuchi S, Sakai T, Kitano A, Takata K, Kinoshita K, Matta Y, Ohtani T, Kimura H, Gabata T. Diagnostic performance of abbreviated gadoxetic acid-enhanced magnetic resonance protocols with contrast-enhanced computed tomography for detection of colorectal liver metastases. *World J Radiol* 2022; 14(10): 352-366

URL: <https://www.wjgnet.com/1949-8470/full/v14/i10/352.htm>

DOI: <https://dx.doi.org/10.4329/wjr.v14.i10.352>

INTRODUCTION

Metastatic disease is the most frequent malignant condition in the liver, and colorectal cancer (CRC), which is the third most common cancer[1], is the most frequent primary cancer causing hepatic metastases. Synchronous and metachronous liver metastases are found in 20%-25% and 35%-55%, respectively, of patients with advanced CRC[2,3]. Accurate detection of metastases is therefore essential for optimizing patient management and guiding therapeutic strategies.

Although several imaging modalities have been adopted to assess hepatic metastases, contrast-enhanced magnetic resonance imaging (MRI) using gadoxetic acid has been shown to offer higher accuracy, sensitivity, and specificity for the detection and characterization of hepatic metastases compared with other modalities such as ultrasound, contrast-enhanced computed tomography (CE-CT), and ¹⁸F-fluoro-2-deoxy-D-glucose positron emission tomography/CT[4-7]. Nevertheless, the long examination time and relatively high cost of the standard MRI protocol with gadoxetic acid limit its use for the routine surveillance of liver metastases in patients with CRC, whereas CE-CT is routinely used for primary staging and metastatic surveillance.

Most previous reports on the detection of liver metastases, including dynamic contrast studies, have assessed acquired sequences[4-7]; however, high sensitivity for the detection of liver metastases is mainly provided by diffusion-weighted imaging (DWI) and hepatobiliary phase (HBP) imaging with gadoxetic acid obtained 20 min after injection[8-10], and no definitive evidence has shown that T1-weighted images with or without fat suppression or dynamic contrast study are essential for accurate detection.

Recently, several selected MRI protocols without dynamic phases [*e.g.*, abbreviated enhanced MRI (Ab-MRI)] have been proposed to achieve equivalent diagnostic performance for the detection of colorectal liver metastases to standard MRI protocols[11-13]. However, the number of reports is still small, and the sequences included in the protocols have been slightly different. As a result, no optimal protocol has been established. Furthermore, while MRI with gadoxetic acid is regularly performed after CE-CT for preoperative CRC staging in clinical settings, no studies appear to have assessed the diagnostic performance of Ab-MRI in combination with CE-CT to determine the best therapeutic strategy.

The purpose of the present study was therefore to compare the diagnostic performance of two Ab-MRI protocols with those of the standard MRI protocol and a combination of an Ab-MRI protocol and CE-CT in the detection of colorectal liver metastases.

MATERIALS AND METHODS

This single-center retrospective study was approved by our institutional review board. Given the retrospective design of the study, the need to obtain written informed consent was waived.

Study population

We identified all patients with CRC pathologically confirmed from surgically resected specimens who had undergone gadoxetic acid-enhanced MRI and CE-CT for cancer staging during the initial work-up between October 2010 and April 2021. In our institution, hepatic MRI using gadoxetic acid and CE-CT are routinely performed during the initial work-up of patients with CRC. The inclusion criteria for the study population were as follows: (1) Pathologically proven primary CRC; (2) performance of CE-CT within 2 wk of an MRI; and (3) previous abdominal CT or MRI performed ≥ 12 mo earlier. Among 386 patients seen in our facility during the study period, 105 patients with CRC confirmed at pathological analysis satisfied the inclusion criteria; 118 patients with CRC had no colorectal liver metastases, and 163 with colorectal liver metastases underwent chemotherapy without surgical resection. Patients with the following conditions were then excluded: motion artifacts or missing part of the MRI acquisition ($n = 5$); history of other malignancy ($n = 4$); missing part of a CT examination due to iodine allergy ($n = 4$); chronic liver disease or cirrhosis ($n = 3$); and cancer other than adenocarcinoma, such as neuroendocrine tumor ($n = 2$). A final total of 87 patients was included in this study (Figure 1). The demographic and clinical-biological data of these patients were obtained from the medical records.

MRI examinations

Gadoxetic acid-enhanced MRI was performed using a 3-T system (Discovery 750 DV 25.1; GE Healthcare, Waukesha, WI, United States) with an 8-channel body phased-array coil. All patients included in the study had undergone scans using a standard liver MRI protocol including the following sequences: in- and opposed-phase T1-weighted imaging, and 3-dimensional T1-weighted fat-suppressed spoiled gradient-recalled echo sequences [liver acquisition with volume acceleration (LAVA); GE Medical Systems] as pre-contrast sequences. After gadoxetic acid (Primovist; Bayer Schering Pharma, Osaka, Japan) was administered at a rate of 1 mL/s followed by a 20-mL saline flush using a power injector and a bolus tracking technique, late arterial-, portal venous-, and transitional-phase images were acquired using LAVA. Single-shot fast spin echo (SSFSE) T2-weighted imaging, fat-suppressed fast spin echo (FSE) T2-weighted imaging, DWI ($b = 0$ s/mm², $b = 800$ s/mm²), and HBP imaging were acquired at least 20 min after contrast administration using the same sequences as applied pre-contrast (Figure 2). Details of the MRI protocols are provided in Table 1.

CT examinations

All CT examinations were conducted using a CT system (SOMATOM Force; Siemens Healthcare, Forchheim, Germany). Following non-enhanced CT, contrast material-enhanced study was performed at 60-70 s (portal phase) and 180 s (equilibrium phase) after completing intravenous injection of non-ionic contrast material (Iopamiron 370; Bayer Health Care, Osaka, Japan) (500 mg of iodine per kilogram body weight) for 30 s. Images were acquired in the craniocaudal direction, including the whole abdomen and pelvis. The following imaging parameters were used: tube current, 250 mAs; tube voltages, 100 kVp; collimation, 0.6 \times 192 mm; pitch factor, 0.8; rotation time, 0.5 s; matrix, 512 \times 512; field of view, 300-500 mm; and reconstruction interval (slice thickness), 3 mm.

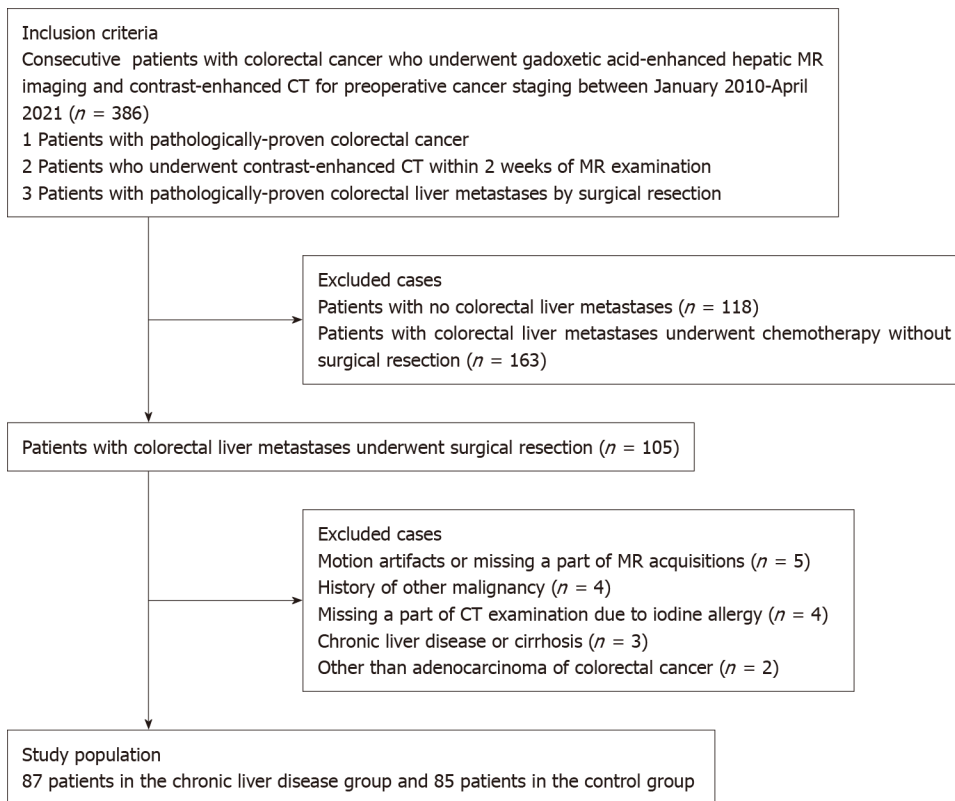
Image analysis

All MRI and CT examinations were pooled after anonymization by a radiologist (K.O.) with 20 years of experience in the field of abdominal imaging who did not participate in the readings. Two different Ab-MRI protocols were arranged, including only SSFSE T2-weighted or fat-suppressed FSE-T2-weighted, DWI and HBP images (Ab-MRI protocol 1 or 2) (Figure 2). Four radiologists (T.S., K.K., K.T., A.K., with 30, 22, 10, and 8 years of experience in oncology imaging, respectively) randomized into two groups retrospectively and independently reviewed the following three reading sessions: (1) Ab-MRI protocol 1

Table 1 Magnetic resonance imaging acquisition parameters

Sequence	Orientation	Respiratory compensation	Repetition/echo time (ms)	Flip angle (degrees)	Section thickness (mm)	Intersection gap (mm)	Field-of-view (mm ²)	Matrix	Acquisition time (s)
T1-weighted in and opposed phases (SPGR)	Axial	Breath-hold	6.9/4.5	12	4	1	350*280	320*224	20
Dynamic study (LAVA) ¹	Axial	Breath-hold	6.5/3.1	15	4	1	350*280	320*192	20
Single-shot FSE T2-weighted imaging	Axial	Breath-hold	520/82	90	5	1	350*350	384*256	20
Diffusion-weighted imaging	Axial	Respiration trigger	8000-12000/68	90	5	1	350*350	128*128	210
Fat-suppressed FSE T2-weighted imaging	Axial	Respiration trigger	520/82	160	5	1	350*350	320*320	230
Hepatobiliary phase	Axial	Breath-hold	6.5/3.1	30	4	1	350*280	320*224	20

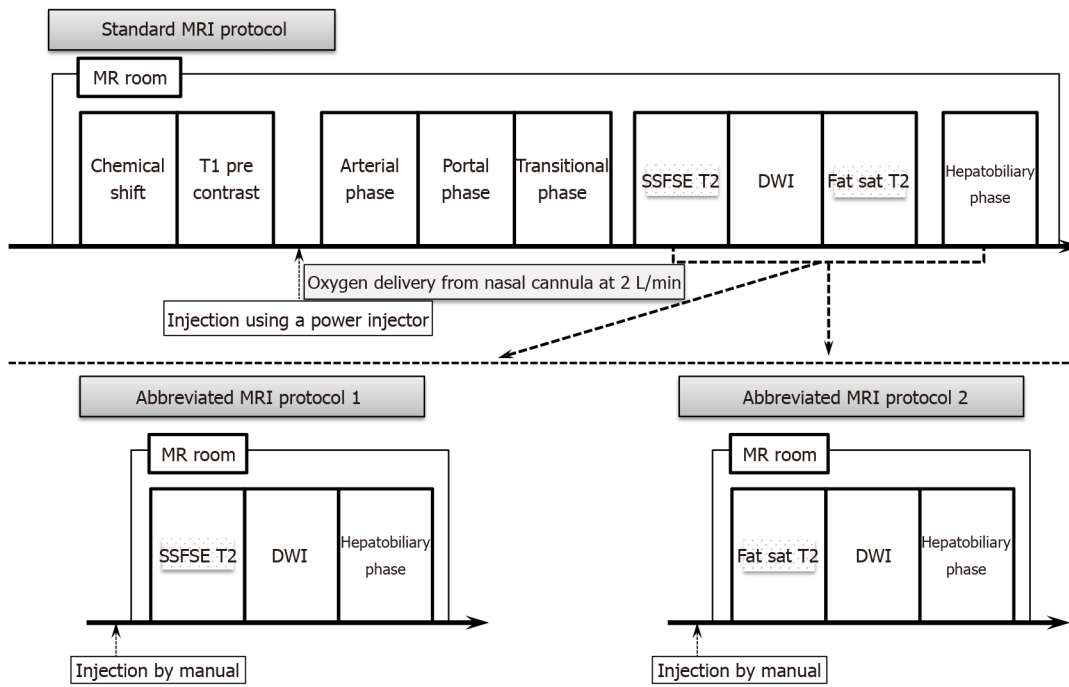
¹Dynamic study consists of pre-contrast, late arterial, portal venous, and transitional phases.
 SPGR: Spoiled gradient-recalled echo; LAVA: Liver acquisition with volume acceleration; FSE: Fast spin echo.



DOI: 10.4329/wjr.v14.i10.352 Copyright ©The Author(s) 2022.

Figure 1 Flowchart of the study population. MR: Magnetic resonance; CT: Computed tomography.

or 2; (2) the standard MRI protocol including all acquired sequences; and (3) a combination of Ab-MRI protocol 1 or 2 and CE-CT. The reader who performed the Ab-MRI in the first reading session used the same abbreviated protocol in the third reading session. All interpretation of images from MRI and CT was blinded to clinical-biological and follow-up data. The reader at the second or third reading was blinded to results from the prior session, which had been held at least 2 mo earlier.



DOI: 10.4329/wjr.v14.i10.352 Copyright ©The Author(s) 2022.

Figure 2 Schematic diagrams of the standard magnetic resonance imaging protocol (upper diagram) and both kinds of simulated abbreviated magnetic resonance imaging protocol (lower diagram). SSFSE T2: Single-shot fast spin echo T2-weighted imaging; Fat-sat T2: Fat-suppressed T2-weighted imaging; DWI: Diffusion-weighted imaging; MR: Magnetic resonance.

Reviewers were asked to report all focal liver lesions detected. Lesion locations were defined according to the Couinaud classification. Maximal diameter on the axial plane was measured in millimeters. Readers characterized the detected lesions using a 5-point scale (1, definitely not liver metastasis; 2, probably not liver metastasis; 3, indeterminate; 4, probably liver metastasis; and 5, definitely liver metastasis). Lesions were considered liver metastases for scores of 4 or 5, whereas lesions were considered to not represent liver metastases for scores ≤ 3 .

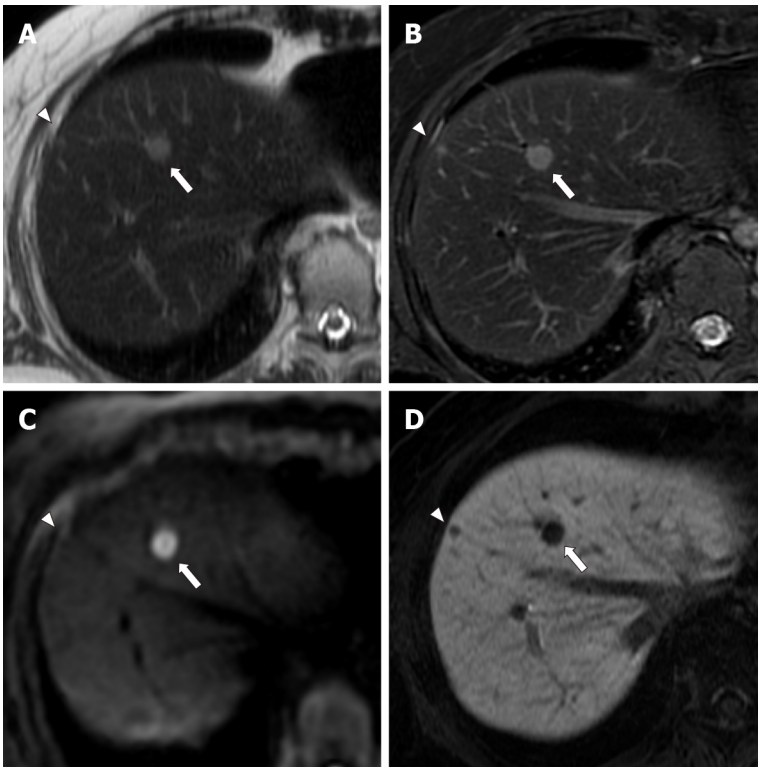
Standard of reference

All metastases were pathologically confirmed from surgically resected specimens. The MRI of each metastasis was pathologically checked in the cut sections of the resected specimens by a radiologist (K.O.) and a pathologist (S.H., 7 years of experience) who did not participate in the readings.

Benign lesions such as simple hepatic cysts and hemangiomas were diagnosed on the basis of typical imaging findings and by the fact that the lesions demonstrated no change in size on previous contrast-enhanced CT or MRI performed over a period of ≥ 12 mo (range, 12-38 mo). Typical imaging findings of hepatic cysts and hemangiomas are as follows: hepatic cysts are diagnosed on the basis of marked hyperintensity on T2-weighted imaging and the absence of contrast enhancement. Hemangiomas are diagnosed on the basis of moderate to marked hyperintensity on T2-weighted imaging and expanding globular peripheral enhancement approximately paralleling that of the blood pool. Tiny hepatic cysts (diameter < 2 mm) detected only on SSFSE T2-weighted imaging were not subjected to analysis. Other benign lesions (such as focal nodular hyperplasia) were also recorded if found. Examples of colorectal liver metastases, hemangiomas, and hepatic cysts are shown in Figures 3-6.

Statistical analysis

Continuous variables are reported as mean and standard or median deviation and extreme values, depending on the distribution. Sensitivity, specificity, positive predictive value (PPV), negative predictive values (NPV), accuracy of each session, and 95% CIs were calculated. A false positive was a lesion considered by radiologists to be malignant but not confirmed as a metastasis according to the reference standard. A false negative was a lesion considered to be benign by radiologists but identified as a metastasis according to the reference standard. McNemar’s test or Fisher’s exact test was used to compare sensitivity, specificity, PPV, NPV, and accuracy between each reading session. Areas under the receiver operating characteristic curve (AUROCs) were computed and compared using the DeLong test. Inter-reader variability for the characterization of detected lesions was assessed using Cohen’s kappa statistics. Kappa values of 0.01-0.20, 0.21-0.40, 0.41-0.60, 0.61-0.80, and 0.81-1.0 were considered to indicate “poor”, “fair”, “moderate”, “good”, and “excellent” agreement, respectively. A bilateral value



DOI: 10.4329/wjr.v14.i10.352 Copyright ©The Author(s) 2022.

Figure 3 A 54-year-old woman with two colorectal liver metastases in segment 8, with diameters of 9 mm (arrows) and 4 mm (arrowheads). A: The larger metastasis (arrow) is clearly depicted as an area of hyperintensity, and the smaller metastasis (arrowhead) shows indistinct hyperintensity on single-shot fast spin echo (SSFSE) imaging; B: Larger (arrow) and smaller (arrowhead) metastases are clearly depicted as an area of hyperintensity on fat-suppressed fast spin echo (FSE) T2-weighted imaging; C: The larger metastasis (arrow) is clearly depicted as an area of hyperintensity, and the smaller metastasis (arrowhead) is not depicted on diffusion-weighted imaging (DWI); D: Larger (arrow) and smaller (arrowhead) metastases are clearly depicted as an area of hypointensity on hepatobiliary-phase imaging. Abbreviated magnetic resonance imaging (Ab-MRI) protocol 1 included SSFSE T2-weighted imaging (A), DWI (C), and hepatobiliary-phase imaging (D), whereas abbreviated MRI protocol 2 included fat-suppressed FSE T2-weighted imaging (B), DWI (C), and hepatobiliary phase imaging (D). The larger metastasis (arrows) were scored as 5 by all four readers. The smaller metastasis (arrowheads) was incorrectly scored as 3 or 4 by one of the two readers in Ab-MRI protocols 1 and 2, respectively, and was missed by one reader in Ab-MRI protocol 1.

of $P < 0.05$ was considered statistically significant. All statistical analyses were performed using SPSS software version 21.0 (SPSS, IBM; Armonk, NY, United States).

RESULTS

Patient and tumor characteristics

The 87 patients had 195 metastases (51.4%) and 175 benign lesions (49.6%) (15 hemangiomas/160 cysts; no other benign lesions were observed). The mean sizes of metastases and benign lesions were 28.2 ± 13.6 mm and 4.8 ± 2.8 mm, and median numbers per patient were 2.2 (range, 1-8) and 3.1 (range, 0-12), respectively. Patient and tumor characteristics are shown in [Table 2](#).

Lesion detection

A total of 352 (95.1%) and 349 (94.3%) of the 370 Lesions were detected by Readers 1 and 2, respectively, using Ab-MRI protocol 1, including 182 (93.3%) and 178 (91.3%) of the 195 metastases and 170 (97.1%) and 171 (97.7%) of the 175 benign lesions, respectively. A total of 350 (94.6%) and 355 (95.9%) of the 370 Lesions were detected by Readers 3 and 4, respectively, using Ab-MRI protocol 2, including 185 (94.9%) and 184 (94.4%) of the 195 metastases and 168 (96.0%) and 171 (97.7%) of the 175 benign lesions, respectively.

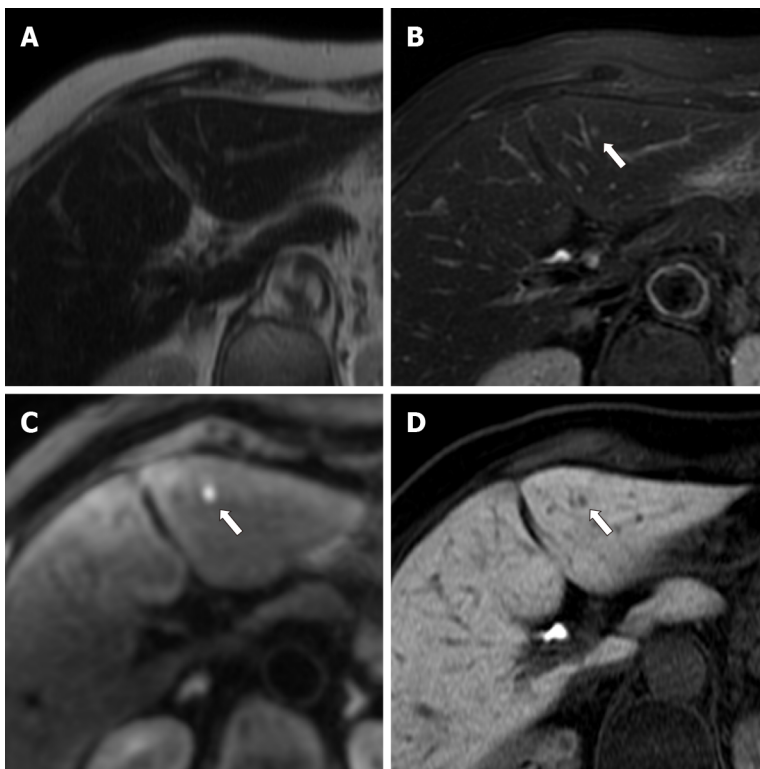
All performance indices (sensitivity, specificity, PPV, NPV, accuracy, and AUROC) for the two Ab-MRI protocols were similar. Sensitivity, specificity, PPV, and NPV of the two Ab-MRI protocols were non-inferior to that of standard MRI for all readers ($P > 0.05$), whereas significant differences in accuracy and AUROC were observed ($P < 0.05$).

All performance indices for the combination of Ab-MRI and CE-CT were higher than that of Ab-MRI alone for all four readers, although only accuracy or AUROC differed significantly ($P < 0.05$). All performance indices for the combination of Ab-MRI and CE-CT were similar to that of standard MRI for

Table 2 Patient and tumor characteristics

Characteristics	
Number of cases	87
Gender (male/female)	51 (58.6%)/36 (41.4%)
Age (yr) ¹ overall	67.2 ± 10.8
Male	67.5 ± 9.6
Female	66.8 ± 12.4
Location of colorectal cancer colon/rectum	31/56
Total number of lesions; metastases/benign	370
Metastases	195 (51.4%)
Benign lesions	175 (49.6%) (15 hemangiomas/160 cysts)
Number of lesions per patient with liver metastases	2.2 (1-8)
Size of metastatic lesion (mm) ¹	28.2 ± 13.6
Number of benign lesions per patient	3.1 (0-12)
Size of benign lesions (mm) ¹	4.8 ± 2.8

¹Data are expressed as means ± SD. Other data represent numbers of lesions and range.



DOI: 10.4329/wjr.v14.i10.352 Copyright ©The Author(s) 2022.

Figure 4 An 86-year-old woman with a colorectal liver metastasis in segment 3, measuring 2.8 mm in diameter (arrows). A: The metastasis (arrow) appears indistinct on single-shot fast spin echo T2-weighted imaging; B: The metastasis (arrow) appears indistinct on fat-suppressed fast spin echo T2-weighted imaging; C: The metastasis (arrow) is clearly depicted as an area of hyperintensity on diffusion-weighted imaging; D: The metastasis (arrow) is clearly depicted as an area of hypointensity on hepatobiliary-phase imaging. The lesion was scored 4 or 5 by one reader in each abbreviated enhanced magnetic resonance imaging (Ab-MRI) protocol, and was missed by the other reader in Ab-MRI protocol 1 and 2.

all four readers ($P > 0.05$). The details and results of a comparison of all performance indices between the three reading sessions by each reader are shown in Tables 3 and 4.

Table 3 Comparison of diagnostic performance of three reading sessions including abbreviated magnetic resonance imaging protocol 1

	Reader 1						Reader 2					
	Ab-MRI	Standard MRI	Ab-MRI + CE-CT	P value (Ab-MRI vs standard)	P value (Ab-MRI vs Ab-MRI + CE-CT)	P value (standard vs Ab-MRI + CE-CT)	Ab-MRI	Standard MRI	Ab-MRI + CE-CT	P value (Ab-MRI vs standard)	P value (Ab-MRI vs Ab-MRI + CE-CT)	P value (standard vs Ab-MRI + CE-CT)
Sensitivity	93.3 (88.9-96.4)	94.4 (92.3-95.1)	93.8 (91.8-94.6)	0.5	> 0.99	> 0.99	91.3 (88.9-92.5)	93.8 (91.7-94.8)	93.3 (91.1-94.3)	0.063	0.125	> 0.99
Specificity	97.1 (93.5-99.1)	98.9 (96.6-99.7)	98.9 (96.6-99.7)	0.125	0.25	> 0.99	97.7 (95.0-99.1)	98.3 (95.8-99.4)	98.3 (95.8-99.4)	> 0.99	> 0.99	> 0.99
PPV	97.3 (93.9-99.1)	98.9 (96.8-99.7)	98.9 (96.8-99.7)	0.25	0.25	> 0.99	97.8 (95.2-99.1)	98.4 (96.1-99.4)	98.4 (96.0-99.4)	0.25	0.25	> 0.99
NPV	92.9 (88.2-96.2)	94 (91.9-94.8)	93.5 (91.4-94.3)	0.5	> 0.99	> 0.99	91 (85.9-94.6)	93.5 (91.2-94.5)	93 (90.6-94.0)	0.063	0.125	> 0.99
Accuracy	95.1 (92.4-97.1)	96.5 (94.4-97.3)	96.2 (94.1-97.0)	0.063	0.125	> 0.99	94.3 (91.8-95.6)	95.9 (93.6-97.0)	95.7 (93.3-96.7)	0.031	0.063	> 0.99
AUROC	0.952 (0.931-0.974)	0.966 (0.948-0.984)	0.964 (0.945-0.982)	0.025	0.045	0.317	0.945 (0.922-0.968)	0.961 (0.941-0.980)	0.958 (0.938-0.978)	0.014	0.025	0.317

Abbreviated magnetic resonance imaging protocol 2 consisting of fat-suppressed fast spin echo T2-weighted, diffusion-weighted, and hepatobiliary phase images. Numbers in square brackets represent 95% CIs. PPV: Positive predictive value; NPV: Negative predictive value; AUROC: Area under the receiver operating characteristic curve; Ab-MRI: Abbreviated magnetic resonance imaging; CE-CT: Contrast-enhanced computed tomography.

More specifically, with regard to false-negative lesions in the Ab-MRI protocols, 11 metastases of the 13 false-negative lesions for reader 1, 12 of 17 for reader 2, 8 of 13 for reader 3, and 6 of 11 for reader 4 were not detected on any of the three reading sessions by each reader, respectively (all were < 1 cm). Among these false-negative lesions, seven metastases were detected by at least one reader using the combination of Ab-MRI and CE-CT or the standard MRI protocol. On the other hand, five small metastases were not detected on any reading sessions by any reader (all were < 1 cm) (Figures 3 and 4). Three of these small metastases were located on the peripheral edge of the liver. The mean diameter of metastases detected using Ab-MRI protocols was 12 ± 10 mm, compared to 2.3 ± 1.7 mm for undetected metastases. With regard to the false-positive lesions, three hemangiomas were misdiagnosed as liver metastases on both Ab-MRI protocols by all four readers and correctly diagnosed on standard MRI and the combination of Ab-MRI and CE-CT (Figure 5).

Inter-reader agreement for tumor classification

In Ab-MRI protocol 1, the kappa value for the two readers was 0.891 (95%CI: 0.846-0.938) for the combination of Ab-MRI and CE-CT, which was slightly higher than that for Ab-MRI (0.849; 95%CI: 0.795-0.903) and standard MRI (0.887; 95%CI: 0.839-0.9334). In Ab-MRI protocol 2, the kappa value for the two readers was 0.935 (95%CI: 0.899-0.971) for the combination of Ab-MRI and CE-CT, which was

Table 4 Comparison of diagnostic performance of three reading sessions including abbreviated magnetic resonance imaging protocol 2

	Reader 3						Reader 4					
	Ab-MRI	Standard MRI	Ab-MRI + CE-CT	P value (Ab-MRI vs standard)	P value (Ab-MRI vs Ab-MRI + CE-CT)	P value (standard vs Ab-MRI + CE-CT)	Ab-MRI	Standard MRI	Ab-MRI + CE-CT	P value (Ab-MRI vs standard)	P value (Ab-MRI vs Ab-MRI + CE-CT)	P value (standard vs Ab-MRI + CE-CT)
Sensitivity	93.3 (90.7-95.0)	94.9 (92.7-95.9)	95.9 (93.8-96.9)	0.25	0.063	0.5	94.4 (90.1-97.2)	95.9 (93.8-96.9)	96.9 (95.1-97.6)	0.25	0.063	0.5
Specificity	96 (93.1-97.8)	98.3 (95.9-99.4)	98.3 (96.0-99.4)	0.125	0.125	> 0.99	97.7 (94.3-99.4)	98.3 (96.0-99.4)	98.9 (96.8-99.7)	> 0.99	0.5	> 0.99
PPV	96.3 (93.6-98.0)	98.4 (96.2-99.4)	98.4 (96.3-99.4)	0.125	0.125	> 0.99	97.9 (94.6-99.4)	98.4 (96.3-99.4)	99 (97.1-99.7)	> 0.99	0.5	> 0.99
NPV	92.8 (90.0-94.6)	94.5 (92.2-95.6)	95.6 (93.3-96.6)	0.5	0.125	0.5	94 (89.4-96.9)	95.6 (93.3-96.6)	96.7 (94.7-97.5)	0.25	0.063	0.5
Accuracy	94.6 (91.9-96.3)	96.5 (94.2-97.5)	97 (94.9-98.0)	0.016	0.004	0.5	95.9 (93.4-97.7)	97 (94.9-98.0)	97.8 (95.9-98.6)	0.125	0.063	0.5
AUROC	0.947 (0.924-0.969)	0.943 (0.919-0.967)	0.948 (0.925-0.971)	0.603	0.862	0.156	0.960 (0.941-0.980)	0.971 (0.954-0.988)	0.979 (0.964-0.993)	0.045	0.007	0.083

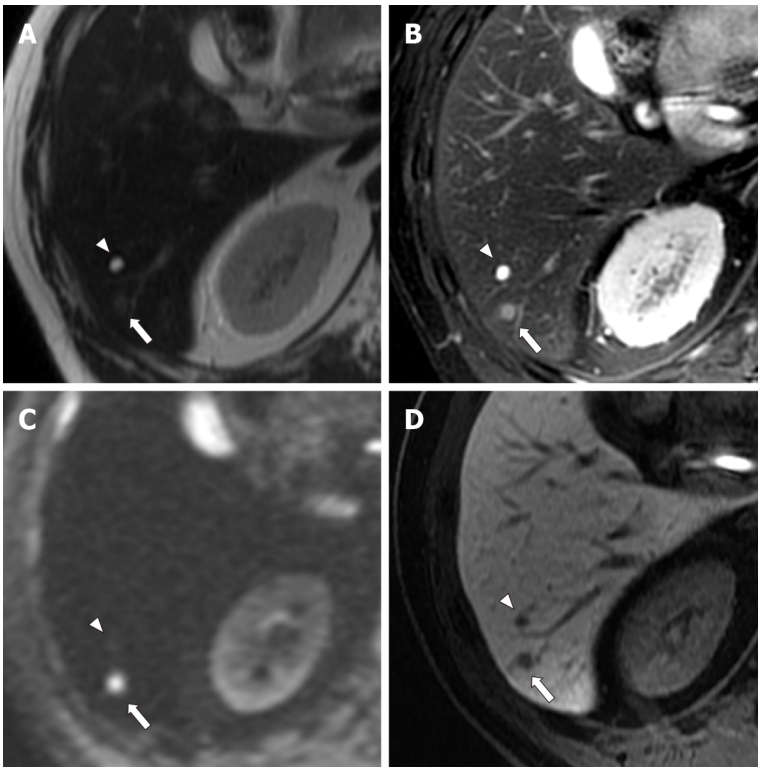
Abbreviated magnetic resonance imaging protocol 2 consisting of fat-suppressed fast spin echo T2-weighted, diffusion-weighted, and hepatobiliary phase images. Numbers in square brackets represent 95% CIs. PPV: Positive predictive value; NPV: Negative predictive value; AUROC: Area under the receiver operating characteristic curve; Ab-MRI: Abbreviated magnetic resonance imaging; CE-CT: Contrast-enhanced computed tomography.

similar to that for standard MRI (0.942; 95%CI: 0.885-0.963) and slightly higher than that for Ab-MRI (0.827; 95%CI: 0.770-0.885). All kappa values indicated excellent inter-reader agreement with regard to the presence of liver metastases.

DISCUSSION

The results of this study revealed that the overall diagnostic performances of both Ab-MRI protocols 1 and 2 were non-inferior to that of the standard MRI protocol, and that of the combination of Ab-MRI and CE-CT were higher than that of Ab-MRI alone and similar to that of the standard MRI protocol. These findings indicate that Ab-MRI protocols could provide a viable alternative to conventional MRI protocols for evaluating colorectal liver metastases, and that parallel assessment with CE-CT appears more useful.

Our results are similar to those from other recently published articles[11,12]. In retrospective studies of patients with CRC and using a similar design, Ghorra *et al*[11] and Canellas *et al*[12] assessed similar Ab-MRI protocols and reported high sensitivity for lesion detection (88.5% and 93.5%, respectively) and



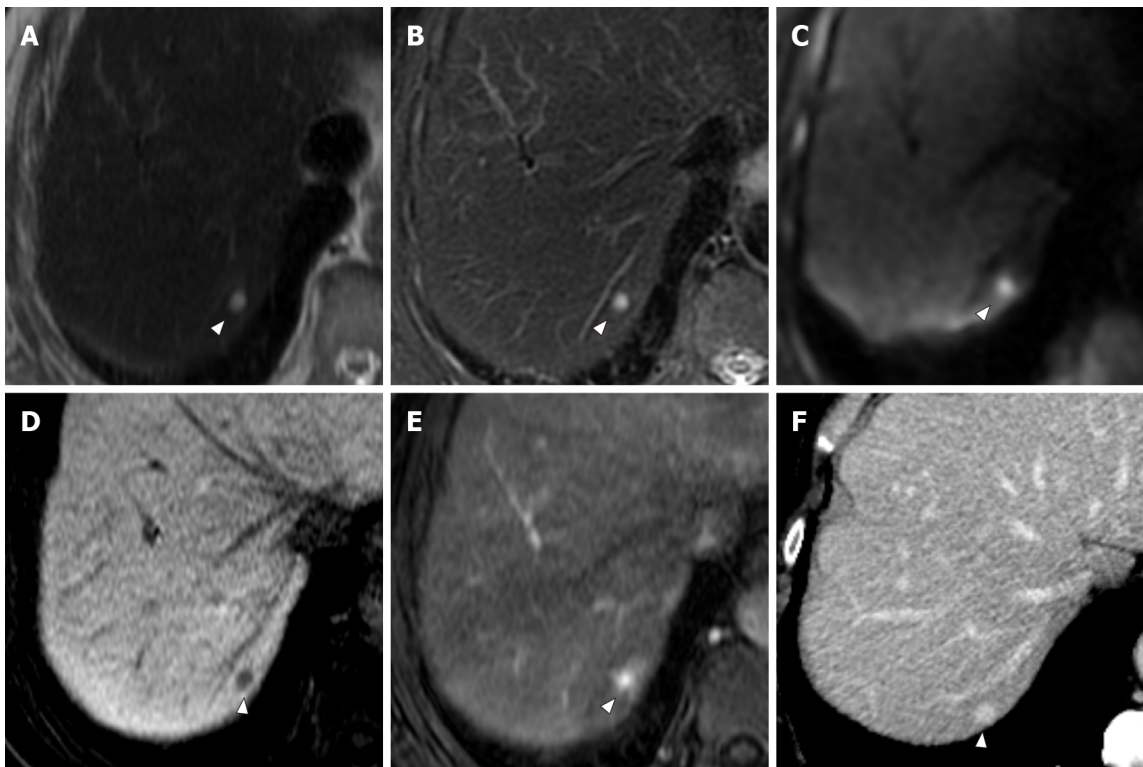
DOI: 10.4329/wjr.v14.i10.352 Copyright ©The Author(s) 2022.

Figure 5 A 59-year-old man with a colorectal small liver metastasis (arrows) and a small simple hepatic cyst (arrowheads) that were 4.1 mm and 5.5 mm, respectively. A: The metastasis (arrow) appears indistinct, whereas the cyst (arrowhead) is clearly depicted as an area of hyperintensity on single-shot fast spin echo T2-weighted imaging; B: The metastasis (arrow) is depicted as mild hyperintensity, and the cyst (arrowhead) is clearly depicted as an area of hyperintensity on fat-suppressed fast spin echo T2-weighted imaging; C: The metastasis (arrow) is clearly depicted as an area of hyperintensity, and the cyst (arrowhead) is not depicted on diffusion-weighted imaging; D: The metastasis (arrow) and the cyst (arrowhead) are clearly depicted as an area of hypointensity on hepatobiliary-phase imaging. The metastasis (arrows) was scored 5 by all four readers. The cyst (arrowheads) was scored 1 or 2 by all four readers.

high PPV for lesion characterization (91.9% and 98.3%, respectively). The high diagnostic performance of Ab-MRI protocols could be preserved with DWI and HBP images[8-10]. Because of the background suppression of normal parenchyma and intrahepatic vessels, DWI shows high sensitivity for detecting liver metastases, especially small lesions < 2 cm in diameter, compared with T2-weighted imaging, and discriminates between metastases and benign lesions more effectively because of its excellent contrast-to-noise ratio (CNR) and signal-to-noise ratio (SNR)[14,15]. Gadoxetic acid-enhanced MRI also shows high sensitivity (92%), particularly for small lesions (≤ 1 cm), even compared with enhanced MRI using superparamagnetic iron oxide (63%)[16]. The higher detection sensitivity of gadoxetic acid-enhanced MRI can be explained by the HBP images, which provide higher SNR, CNR, and spatial resolution, improving the conspicuity and detectability of liver metastases[17,18]. The combination of DWI and HBP images yield excellent performance for lesion detection compared with each sequence alone[9,10]. However, these two sequences are insufficient for the accurate detection and diagnosis of liver metastases.

DWI characterization of focal liver lesions offers several potential pitfalls and limitations. First, the DWI signal intensity for metastases shows significant overlap between those of benign and other malignant lesions[19], and cannot accurately distinguish between each focal liver lesion. In addition, DWI in the upper abdomen is limited by susceptibility and ghosting artifacts in relation to the presence of gas in the nearby bowel and physiologic movements, respectively, which can hide lesions located on the upper edge or in the left lobe, respectively[15,20,21]. The excellent detectability of HBP images can compensate for these limitations but because many types of lesions show the same hypointensity, HBP images without dynamic contrast also show a potential drawback in regard to the difficulty of characterizing focal hepatic lesions.

Lesion characterization requires additional sequences, mainly for differentiating between metastases and benign lesions such as cysts or hemangiomas. We therefore adopted T2-weighted images in the present study, as with previous reports[11-13]. On T2-weighted imaging, liver metastases tend to show mild hyperintensity compared with cysts and hemangiomas, both of which show marked hyperintensity[22]. SSFSE T2-weighted imaging is more useful than FSE T2-weighted imaging for characterizing cysts and hemangiomas[23], whereas liver metastases (particularly small lesions) remain indistinct. On the other hand, FSE T2-weighted imaging with fat suppression might be more helpful for differentiating metastases from hemangiomas[24]. As both SSFSE and FSE T2-weighted imaging have specific



DOI: 10.4329/wjr.v14.i10.352 Copyright ©The Author(s) 2022.

Figure 6 A 70-year-old man with colorectal liver metastasis (not shown) and a hepatic hemangioma in segment 7, which is 4 mm in diameter (arrowheads). A: The hemangioma (arrowhead) is clearly depicted as an area of hyperintensity on single-shot fast spin echo T2-weighted imaging; B: The hemangioma (arrowhead) is clearly depicted as an area of hyperintensity on fat-suppressed fast spin echo T2-weighted imaging; C: The hemangioma (arrowhead) is clearly depicted as an area of hyperintensity on diffusion-weighted imaging; D: The hemangioma (arrowhead) is clearly depicted as an area of hypointensity on hepatobiliary-phase imaging; E: The characteristic early enhancement accompanying arterio-portal shunt of hemangioma (arrowhead) is depicted on arterial phase magnetic resonance (MR) image; F: The characteristic prolonged enhancement of hemangioma (arrowhead) is depicted on equilibrium phase computed tomography (CT) image. The lesion was incorrectly scored 4 by two readers in abbreviated enhanced magnetic resonance imaging (Ab-MRI) protocol 1, and was scored 4 or 5 by two readers in Ab-MRI protocol 2. The lesion was scored 1 by all four readers in standard MR protocol and the combination of each Ab-MRI and contrast-enhanced CT.

advantages and disadvantages, we used two kinds of Ab-MRI protocol including T2-weighted imaging. Consequently, our results showed little difference between both kinds of Ab-MRI protocols with SSFSE or FSE T2-weighted images.

The difficulties in discriminating between metastases and hemangiomas, particularly for small lesions, may be a potential drawback of even gadoxetic acid-enhanced MRI, including dynamic contrast study, which is the standard protocol, because of the lack of an equilibrium phase in the real sense of the term[25,26]. The shortcomings of gadoxetic acid-enhanced MRI can be overcome by CE-CT, as supported by Sofue's report[27] that the PPV with the combination of CE-CT and gadoxetic acid-enhanced MRI was superior to that of gadoxetic acid-enhanced MRI alone[4,17,28]. To the best of our knowledge, this study provides the first assessment of the diagnostic performance of combination CE-CT and Ab-MRI for liver metastases. CT examinations are required to determine the therapeutic strategy for CRC. The use of CT examinations in Ab-MRI reading sessions is thus quite reasonable. Our results revealed that the combination of CE-CT and Ab-MRI achieved superior detection and characterization performance compared with Ab-MRI alone, and were quite similar to standard MRI alone[4,17,28].

Ab-MRI protocols should enable a reduction in imaging acquisition time, as noted by Canellas *et al* [12], who reported that Ab-MRI protocols may be performed in less than 15 min, while standard liver MRI takes up to 30 min. The implementation of Ab-MRI protocols can be expected because they have shown no significant influence on gadoxetic acid administration on T2-weighted imaging and diffusion sequences in regard to acquisition and image interpretation[29,30], suggesting that patients could undergo contrast administration without a bolus injection before entering the MRI suite. This would not only reduce the imaging acquisition time, but also provide several other advantages. First, a smaller intravenous route could be used because of the absence of a bolus injection, and this could reduce complications such as the leakage of contrast materials. Second, avoiding the use of a power injector could allow tangled procedures to be limited. Third, saline solution would not be needed after administration of gadoxetic acid, which would cut costs. Fourth, oxygen administration, which is used in selected patients to obtain appropriate arterial-phase images, would be unnecessary, resulting in

additional cost-cutting. Fifth, fewer imaging sequences would be needed, which would save time.

This study has several limitations that need to be considered. First, the study used a retrospective design and included a relatively small number of patients from a single center. Second, selection bias was possible because the patients selected for our series all had a high probability of metastases being detected, owing to our aim to achieve histologic diagnostic confirmation. Third, despite their availability as additional data, we did not assess apparent diffusion coefficient maps or values. Fourth, given the retrospective nature of this study, we could not measure the true acquisition time or cost of the Ab-MRI protocols. Fifth, unexpected malignant lesions other than colorectal liver metastases, such as hepatocellular carcinoma, could not be accurately diagnosed. Sixth, no other metastatic sites were assessed, because this study focused only on liver tumors. Finally, we did not assess the influence of the MRI protocol on surgical management or patient survival. Overall, further analyses are warranted before deciding whether to adapt Ab-MRI protocols for the initial surveillance of liver metastases in patients with CRC.

CONCLUSION

The diagnostic performances of two kinds of Ab-MRI protocol, including SSFSE or FSE T2-weighted images, were non-inferior to that of the standard protocol. The combination of Ab-MRI and CE-CT provided better diagnostic performance than Ab-MRI alone, nearly equivalent to that of the standard protocol.

ARTICLE HIGHLIGHTS

Research background

Although contrast-enhanced magnetic resonance imaging (MRI) using gadoxetic acid has been shown to have higher accuracy, sensitivity, and specificity for the detection and characterization of hepatic metastases compared with other modalities, the long examination time would limit the broad indication. Several abbreviated MRI protocols without dynamic phases (Ab-MRI) have been proposed to achieve equivalent diagnostic performance for the detection of colorectal liver metastases. However, an optimal protocol has not been established, and no studies have assessed the diagnostic performance of Ab-MRI combined with contrast-enhanced computed tomography (CE-CT), which is the preoperative imaging of colorectal cancer staging in clinical settings, to determine the best therapeutic strategy.

Research motivation

The long examination time and relatively high cost of the standard MRI protocol with gadoxetic acid limit its use for the routine surveillance of liver metastases in patients with colorectal cancer. In order to further expand use of the MRI examination with gadoxetic acid with maintaining the diagnostic performance of liver metastases in patients with colorectal cancer, the diagnostic performance of Ab-MRI combined with or without CE-CT, which is the preoperative imaging of colorectal cancer should be estimated.

Research objectives

To compare the diagnostic performance of two kinds of Ab-MRI protocol with the standard MRI protocol and a combination of the Ab-MRI protocol and CE-CT for the detection of colorectal liver metastases.

Research methods

Study participants comprised 87 patients (51 males, 36 females; mean age, 67.2 ± 10.8 years) who had undergone gadoxetic acid-enhanced MRI and CE-CT during the initial work-up for colorectal cancer from 2010 to 2021. Each exam was independently reviewed by two readers in three reading sessions: (1) Only single-shot fast spin echo (FSE) T2-weighted or fat-suppressed-FSE-T2-weighted, diffusion-weighted, and hepatobiliary-phase images (Ab-MRI protocol 1 or 2); (2) all acquired MRI sequences (standard protocol); and (3) a combination of an Ab-MRI protocol (1 or 2) and CE-CT. Diagnostic performance was then statistically analyzed.

Research results

A total of 380 Lesions were analyzed, including 195 metastases (51.4%). Results from the two Ab-MRI protocols were similar. The sensitivity, specificity, and positive and negative predictive values from Ab-MRI were non-inferior to those from standard MRI ($P > 0.05$), while those from the combination of Ab-MRI protocol and CE-CT tended to be higher than those from Ab-MRI alone, although the difference was not significant ($P > 0.05$), and were quite similar to those from standard MRI ($P > 0.05$).

Research conclusions

The diagnostic performances of two kinds of Ab-MRI protocol, including SSFSE or FSE T2-weighted images, were non-inferior to that of the standard protocol. The combination of Ab-MRI and CE-CT provided better diagnostic performance than Ab-MRI alone, nearly equivalent to that of the standard protocol.

Research perspectives

The combination of Ab-MRI and CE-CT can provide a sufficient diagnostic performance for the detection of colorectal liver metastases, and enable a reduction in imaging acquisition time.

FOOTNOTES

Author contributions: Ozaki K contributed to the methodology and data curation; Ishida S contributed to the conceptualization; Higuchi S, Sakai T, Kitano A, Takata K and Kinoshita K contributed to the investigation; Ozaki K, Matta Y and Ohtani T contributed to the writing-original draft; Kimura H contributed to the methodology, writing-review and editing; Gabata T contributed to the supervision and project administration.

Institutional review board statement: This single-center retrospective study was approved by our institutional review board (No. 20210035).

Informed consent statement: The written informed consent was waived.

Conflict-of-interest statement: The authors declare that they have no conflicts of interest.

Data sharing statement: The authors share all data.

Open-Access: This article is an open-access article that was selected by an in-house editor and fully peer-reviewed by external reviewers. It is distributed in accordance with the Creative Commons Attribution NonCommercial (CC BY-NC 4.0) license, which permits others to distribute, remix, adapt, build upon this work non-commercially, and license their derivative works on different terms, provided the original work is properly cited and the use is non-commercial. See: <https://creativecommons.org/licenses/by-nc/4.0/>

Country/Territory of origin: Japan

ORCID number: Kumi Ozaki [0000-0002-1454-7512](https://orcid.org/0000-0002-1454-7512); Shota Ishida [0000-0002-0728-8057](https://orcid.org/0000-0002-0728-8057); Shohei Higuchi [0000-0002-5301-1390](https://orcid.org/0000-0002-5301-1390); Ayaki Kitano [0000-0001-8704-3465](https://orcid.org/0000-0001-8704-3465); Yuki Matta [0000-0003-4338-0771](https://orcid.org/0000-0003-4338-0771); Takashi Ohtani [0000-0002-7318-4571](https://orcid.org/0000-0002-7318-4571); Hirohiko Kimura [0000-0003-1649-2030](https://orcid.org/0000-0003-1649-2030); Toshifumi Gabata [0000-0002-9413-3431](https://orcid.org/0000-0002-9413-3431).

S-Editor: Zhang H

L-Editor: A

P-Editor: Zhang H

REFERENCES

- 1 **Haggard FA**, Boushey RP. Colorectal cancer epidemiology: incidence, mortality, survival, and risk factors. *Clin Colon Rectal Surg* 2009; **22**: 191-197 [PMID: [21037809](https://pubmed.ncbi.nlm.nih.gov/21037809/) DOI: [10.1055/s-0029-1242458](https://doi.org/10.1055/s-0029-1242458)]
- 2 **Siegel R**, Ma J, Zou Z, Jemal A. Cancer statistics, 2014. *CA Cancer J Clin* 2014; **64**: 9-29 [PMID: [24399786](https://pubmed.ncbi.nlm.nih.gov/24399786/) DOI: [10.3322/caac.21208](https://doi.org/10.3322/caac.21208)]
- 3 **Seront E**, Van den Eynde M. Liver-directed therapies: does it make sense in the current therapeutic strategy for patients with confined liver colorectal metastases? *Clin Colorectal Cancer* 2012; **11**: 177-184 [PMID: [22306027](https://pubmed.ncbi.nlm.nih.gov/22306027/) DOI: [10.1016/j.clcc.2011.12.004](https://doi.org/10.1016/j.clcc.2011.12.004)]
- 4 **Scharitzer M**, Ba-Ssalamah A, Ringl H, Kölblinger C, Grünberger T, Weber M, Schima W. Preoperative evaluation of colorectal liver metastases: comparison between gadoteric acid-enhanced 3.0-T MRI and contrast-enhanced MDCT with histopathological correlation. *Eur Radiol* 2013; **23**: 2187-2196 [PMID: [23519439](https://pubmed.ncbi.nlm.nih.gov/23519439/) DOI: [10.1007/s00330-013-2824-z](https://doi.org/10.1007/s00330-013-2824-z)]
- 5 **Cho JY**, Lee YJ, Han HS, Yoon YS, Kim J, Choi Y, Shin HK, Lee W. Role of gadoteric acid-enhanced magnetic resonance imaging in the preoperative evaluation of small hepatic lesions in patients with colorectal cancer. *World J Surg* 2015; **39**: 1161-1166 [PMID: [25609116](https://pubmed.ncbi.nlm.nih.gov/25609116/) DOI: [10.1007/s00268-015-2944-5](https://doi.org/10.1007/s00268-015-2944-5)]
- 6 **Kim HJ**, Lee SS, Byun JH, Kim JC, Yu CS, Park SH, Kim AY, Ha HK. Incremental value of liver MR imaging in patients with potentially curable colorectal hepatic metastasis detected at CT: a prospective comparison of diffusion-weighted imaging, gadoteric acid-enhanced MR imaging, and a combination of both MR techniques. *Radiology* 2015; **274**: 712-722 [PMID: [25286324](https://pubmed.ncbi.nlm.nih.gov/25286324/) DOI: [10.1148/radiol.14140390](https://doi.org/10.1148/radiol.14140390)]
- 7 **Floriani I**, Torri V, Rulli E, Garavaglia D, Compagnoni A, Salvolini L, Giovagnoni A. Performance of imaging modalities in diagnosis of liver metastases from colorectal cancer: a systematic review and meta-analysis. *J Magn Reson Imaging* 2010; **31**: 19-31 [PMID: [20027569](https://pubmed.ncbi.nlm.nih.gov/20027569/) DOI: [10.1002/jmri.22010](https://doi.org/10.1002/jmri.22010)]

- 8 **Colagrande S**, Castellani A, Nardi C, Lorini C, Calistri L, Filippone A. The role of diffusion-weighted imaging in the detection of hepatic metastases from colorectal cancer: A comparison with unenhanced and Gd-EOB-DTPA enhanced MRI. *Eur J Radiol* 2016; **85**: 1027-1034 [PMID: 27130067 DOI: 10.1016/j.ejrad.2016.02.011]
- 9 **Vilgrain V**, Esvan M, Ronot M, Caumont-Prim A, Aubé C, Chatellier G. A meta-analysis of diffusion-weighted and gadoxetic acid-enhanced MR imaging for the detection of liver metastases. *Eur Radiol* 2016; **26**: 4595-4615 [PMID: 26883327 DOI: 10.1007/s00330-016-4250-5]
- 10 **Koh DM**, Collins DJ, Wallace T, Chau I, Riddell AM. Combining diffusion-weighted MRI with Gd-EOB-DTPA-enhanced MRI improves the detection of colorectal liver metastases. *Br J Radiol* 2012; **85**: 980-989 [PMID: 22167501 DOI: 10.1259/bjr/91771639]
- 11 **Ghorra C**, Pommier R, Piveteau A, Rubbia-Brandt L, Vilgrain V, Terraz S, Ronot M. The diagnostic performance of a simulated "short" gadoxetic acid-enhanced MRI protocol is similar to that of a conventional protocol for the detection of colorectal liver metastases. *Eur Radiol* 2021; **31**: 2451-2460 [PMID: 33025173 DOI: 10.1007/s00330-020-07344-0]
- 12 **Canellas R**, Patel MJ, Agarwal S, Sahani DV. Lesion detection performance of an abbreviated gadoxetic acid-enhanced MRI protocol for colorectal liver metastasis surveillance. *Eur Radiol* 2019; **29**: 5852-5860 [PMID: 30888485 DOI: 10.1007/s00330-019-06113-y]
- 13 **Granata V**, Fusco R, Avallone A, Cassata A, Palaia R, Delrio P, Grassi R, Tatangelo F, Grazzini G, Izzo F, Petrillo A. Abbreviated MRI protocol for colorectal liver metastases: How the radiologist could work in pre surgical setting. *PLoS One* 2020; **15**: e0241431 [PMID: 33211702 DOI: 10.1371/journal.pone.0241431]
- 14 **Parikh T**, Drew SJ, Lee VS, Wong S, Hecht EM, Babb JS, Taouli B. Focal liver lesion detection and characterization with diffusion-weighted MR imaging: comparison with standard breath-hold T2-weighted imaging. *Radiology* 2008; **246**: 812-822 [PMID: 18223123 DOI: 10.1148/radiol.2463070432]
- 15 **Coenegrachts K**, Delanote J, Ter Beek L, Haspelslagh M, Bipat S, Stoker J, Van Kerkhove F, Steyaert L, Rigauts H, Casselman JW. Improved focal liver lesion detection: comparison of single-shot diffusion-weighted echoplanar and single-shot T2 weighted turbo spin echo techniques. *Br J Radiol* 2007; **80**: 524-531 [PMID: 17510250 DOI: 10.1259/bjr/33156643]
- 16 **Muhi A**, Ichikawa T, Motosugi U, Sou H, Nakajima H, Sano K, Sano M, Kato S, Kitamura T, Fatima Z, Fukushima K, Iino H, Mori Y, Fujii H, Araki T. Diagnosis of colorectal hepatic metastases: comparison of contrast-enhanced CT, contrast-enhanced US, superparamagnetic iron oxide-enhanced MRI, and gadoxetic acid-enhanced MRI. *J Magn Reson Imaging* 2011; **34**: 326-335 [PMID: 21780227 DOI: 10.1002/jmri.22613]
- 17 **Sofue K**, Tsurusaki M, Tokue H, Arai Y, Sugimura K. Gd-EOB-DTPA-enhanced 3.0 T MR imaging: quantitative and qualitative comparison of hepatocyte-phase images obtained 10 min and 20 min after injection for the detection of liver metastases from colorectal carcinoma. *Eur Radiol* 2011; **21**: 2336-2343 [PMID: 21748389 DOI: 10.1007/s00330-011-2197-0]
- 18 **Chang KJ**, Kamel IR, Macura KJ, Bluemke DA. 3.0-T MR imaging of the abdomen: comparison with 1.5 T. *Radiographics* 2008; **28**: 1983-1998 [PMID: 19001653 DOI: 10.1148/rg.287075154]
- 19 **Wei C**, Tan J, Xu L, Juan L, Zhang SW, Wang L, Wang Q. Differential diagnosis between hepatic metastases and benign focal lesions using DWI with parallel acquisition technique: a meta-analysis. *Tumour Biol* 2015; **36**: 983-990 [PMID: 25318600 DOI: 10.1007/s13277-014-2663-9]
- 20 **Chen ZG**, Xu L, Zhang SW, Huang Y, Pan RH. Lesion discrimination with breath-hold hepatic diffusion-weighted imaging: a meta-analysis. *World J Gastroenterol* 2015; **21**: 1621-1627 [PMID: 25663782 DOI: 10.3748/wjg.v21.i5.1621]
- 21 **Xiong H**, Zeng YL. Standard-b-Value Versus Low-b-Value Diffusion-Weighted Imaging in Hepatic Lesion Discrimination: A Meta-analysis. *J Comput Assist Tomogr* 2016; **40**: 498-504 [PMID: 26938696 DOI: 10.1097/RCT.0000000000000377]
- 22 **Danet IM**, Semelka RC, Braga L, Armao D, Woosley JT. Giant hemangioma of the liver: MR imaging characteristics in 24 patients. *Magn Reson Imaging* 2003; **21**: 95-101 [PMID: 12670595 DOI: 10.1016/s0730-725x(02)00641-0]
- 23 **Kiryu S**, Okada Y, Ohtomo K. Differentiation between hemangiomas and cysts of the liver with single-shot fast-spin echo image using short and long TE. *J Comput Assist Tomogr* 2002; **26**: 687-690 [PMID: 12439299 DOI: 10.1097/00004728-200209000-00004]
- 24 **Takayama Y**, Nishie A, Okamoto D, Fujita N, Asayama Y, Ushijima Y, Yoshizumi T, Yoneyama M, Ishigami K. Differentiating Liver Hemangioma from Metastatic Tumor Using T2-enhanced Spin-echo Imaging with a Time-reversed Gradient-echo Sequence in the Hepatobiliary Phase of Gadoxetic Acid-enhanced MR Imaging. *Magn Reson Med Sci* 2022; **21**: 445-457 [PMID: 33883364 DOI: 10.2463/mrms.mp.2020-0151]
- 25 **Tateyama A**, Fukukura Y, Takumi K, Shindo T, Kumagae Y, Kamimura K, Nakajo M. Gd-EOB-DTPA-enhanced magnetic resonance imaging features of hepatic hemangioma compared with enhanced computed tomography. *World J Gastroenterol* 2012; **18**: 6269-6276 [PMID: 23180948 DOI: 10.3748/wjg.v18.i43.6269]
- 26 **Goshima S**, Kanematsu M, Watanabe H, Kondo H, Shiratori Y, Onozuka M, Moriyama N. Hepatic hemangioma and metastasis: differentiation with gadoxetate disodium-enhanced 3-T MRI. *AJR Am J Roentgenol* 2010; **195**: 941-946 [PMID: 20858822 DOI: 10.2214/AJR.09.3730]
- 27 **Sofue K**, Tsurusaki M, Murakami T, Onoe S, Tokue H, Shibamoto K, Arai Y, Sugimura K. Does Gadoxetic acid-enhanced 3.0T MRI in addition to 64-detector-row contrast-enhanced CT provide better diagnostic performance and change the therapeutic strategy for the preoperative evaluation of colorectal liver metastases? *Eur Radiol* 2014; **24**: 2532-2539 [PMID: 24865698 DOI: 10.1007/s00330-014-3233-7]
- 28 **Berger-Kulemann V**, Schima W, Baroud S, Koelblinger C, Kaczirek K, Gruenberger T, Schindl M, Maresch J, Weber M, Ba-Ssalamah A. Gadoxetic acid-enhanced 3.0 T MR imaging versus multidetector-row CT in the detection of colorectal metastases in fatty liver using intraoperative ultrasound and histopathology as a standard of reference. *Eur J Surg Oncol* 2012; **38**: 670-676 [PMID: 22652037 DOI: 10.1016/j.ejso.2012.05.004]
- 29 **Choi SA**, Lee SS, Jung IH, Kim HA, Byun JH, Lee MG. The effect of gadoxetic acid enhancement on lesion detection and characterisation using T₂ weighted imaging and diffusion weighted imaging of the liver. *Br J Radiol* 2012; **85**: 29-36 [PMID: 21123305 DOI: 10.1259/bjr/12929687]

- 30 **Cieszanowski A**, Podgórska J, Rosiak G, Maj E, Grudziński IP, Kaczyński B, Szeszkowski W, Milczarek K, Rowiński O. Gd-EOB-DTPA-Enhanced MR Imaging of the Liver: The Effect on T2 Relaxation Times and Apparent Diffusion Coefficient (ADC). *Pol J Radiol* 2016; **81**: 103-109 [PMID: [27026795](#) DOI: [10.12659/PJR.895701](#)]



Published by **Baishideng Publishing Group Inc**
7041 Koll Center Parkway, Suite 160, Pleasanton, CA 94566, USA
Telephone: +1-925-3991568
E-mail: bpgoffice@wjgnet.com
Help Desk: <https://www.f6publishing.com/helpdesk>
<https://www.wjgnet.com>

